TWO-PHASE COUNTERCURRENT FLOW THROUGH A BED OF PACKING. IX.*

THE DIAGRAM OF REGIMES IN TRICKLE AND BUBBLE FLOW BEDS

Z.Brož and V.Kolář

Institute of Chemical Process Fundamentals,
Czechoslovak Academy of Sciences, Prague 6 - Suchdol

Received March 10th, 1972

A diagram of regimes was devised and an analysis was given of a two-phase counter-current flow of gas and liquid in a bed of packing under trickle and bubble flow. It was found that the various forms of expressions for the two-phase pressure drop in trickle and bubble flow beds are particular solutions of the general equation of the flow of liquid and gas through a bed of packing.

This paper is an attempt to generalize the results obtained in the study of trickle beds[1-8] and to unify description of principal hydrodynamic characteristics of trickle and bubble flow beds.

THEORETICAL

A Bed of Packing Under Trickle Flow

The earlier published[1] theoretical analysis of a two-phase counter-current trickle flow in a bed of packing was to provide a unified description of the process based on general laws of motion of fluids with suitably selected empirical coefficients[1] in the whole range of variables starting from zero flow rates of phases up to flooding.

Under acceptable assumptions the analysis[1] lead to a balance of vertical components of forces acting on a stream of liquid in a unit volume of the column in the following form

$$\Delta P_g/l + \Delta P_l/l + \Delta P_s/l = \varrho_l g\,, \qquad (1)$$

$$\Delta P_g/l = \psi_g(G_g^2/[2\varrho_g d_e(e - z)^3])\,, \qquad (2)$$

$$\Delta P_l/l = \psi_l(G_l^2/2\varrho_l d_e z^3)\,, \quad \Delta P_s/l = (1 - \varphi)\,\varrho_l g\,. \qquad (3), (4)$$

The first term on the right hand side of Eq. (*1*), $\Delta P_g/l$, denotes the pressure force of the gas acting on liquid. This force is expressed in Eq. (*2*) in a usual manner by means of the velocity of gas in a bed of equivalent diameter of the gas stream, $d_{eg} = d_e(e - z)$, and the friction factor,

* Part VIII: This Journal *32*, 3551 (1972).

ψ_g. The second term, $\Delta P_l/l$, denotes the friction force acting between the liquid and the surface of the packing plus the interfacial gas–liquid friction. The latter is given in Eq. (3) also in terms of the velocity of liquid, equivalent diameter of the liquid stream, $d_{el} = d_e z$, and the friction factor ψ_l. The third term, $\Delta P_s/l$, formally expressed in Eq. (4) by means of the coefficient φ, denotes the volume forces of liquid transmitted onto the packing (and the grid) either directly or by the surface tension forces acting between the liquid and the surface of the packing. $\Delta P_s/l$ is a function of gas and liquid flow rates, the geometry of packing and the surface forces. At zero velocity of liquid, for instance, this term represents the static hold-up. All participating forces are related to the area of cross-section occupied by liquid hold-up, z. The term on the right hand side of Eq. (1) expresses the volume forces acting on the liquid and it is also related to the cross-section of hold-up. From the above it is apparent that the coefficients ψ_g and ψ_l possess the meaning of friction factors and their value may be determined only in case of a single-phase flow of gas or liquid through the whole cross-section from *e.g.* the Ergun equation[11]. By substituting Eqs (2)—(4) into (1) one obtains a relation for the dependence of liquid hold-up on the mass velocities of gas and liquid in the form[1]

$$\frac{2g\varrho_l^2 d_e z^3}{G_l^2} = \frac{\psi_l}{\varphi} + \frac{\psi_g}{\varphi}\left(\frac{G_g}{G_l}\right)^2 \frac{\varrho_l}{\varrho_g}\left(\frac{z}{e-z}\right)^3 . \tag{5}$$

From this analysis it follows that gas pressure drop and liquid hold-up may be expressed in terms of three coefficients ψ_g, ψ_l and φ, which have to be determined empirically. By processing an extensive set of experimental data[2-8] on liquid hold-up and gas pressure drop with the gas flow rate ranging from zero up to flooding and in a wide range of liquid flow rates, physical properties of liquid, the diameter and geometric shape of packing we have found that: *1)* The dependence of the friction factor ψ_g on gas Reynolds number computed from Eq. (2) for a given flow rate of liquid is very complex and cannot be expressed analytically by simple means[3]. *2)* For a given flow rate of liquid, however, one can delimit two regions of gas mass velocities: A region below ($0 \leqq G_g \leqq G_{gk}$) and above ($G_{gk} \leqq G_g \leqq G_{gz}$) the loading point within which the pressure drop has a satisfactory linear course[3,5] in terms of the variables of Eqs (6) and (7),

$$\frac{\Delta P_g}{\varrho_l l g} = \varphi - \psi_l \frac{G_l^2}{2g\varrho_l^2 d_e z^3} , \tag{6}$$

$$\frac{\Delta P_g}{\varrho_l l g} = \frac{\xi G_g^2}{2g\varrho_l \varrho_g d_e (e-z)^3} + \frac{\zeta}{\varrho_l l g} . \tag{7}$$

This suggests that the coefficients φ and ψ_l, or ξ and ζ, are independent of gas mass velocity and in given regions may be determined empirically. Eq. (6) was obtained by substituting Eqs (3) and (4) into (1); Eq. (7) was found empirically. At low liquid flow rates $\zeta < 0$, for intermediate rates $\zeta = 0$ and for high flow rates $\zeta > 0$. *3)* From the linear dependence of the pressure drop in terms of the variables of Eqs (6) and (7) it further follows the empirical finding that the relation of liquid hold-up and gas mass velocity may be written in terms of the variables of Eq. (5) in the following form[3]

$$\frac{2g\varrho_l^2 d_e z^3}{G_l^2} = \vartheta + \eta\left(\frac{G_g}{G_l}\right)^2 \frac{\varrho_l}{\varrho_g}\left(\frac{z}{e-z}\right)^3 , \tag{8}$$

where the coefficients ϑ and η are constants independent of gas mass velocity within the given range and may be evaluated from experimental data or calculated from the coefficients φ, ψ_l, ξ

and ζ (ref.[5]). The relation between liquid hold-up and gas mass velocity in variables of Eq. (*8*) in the region $G_{gk} \leqq G_g \leqq G_{gz}$ then enables one to derive a limiting condition of flooding in the form[1,4,8] (provided $dG_{gz}/dz = 0$)

$$\left(\frac{\eta G_g^2 z}{2g\varrho_l \varrho_g d_e e^3}\right)^{1/4} + \left(\frac{\vartheta G_l^2}{2g\varrho_l^2 d_e e^3}\right)^{1/4} = 1 . \tag{9}$$

The next step of the analysis was a search for a suitable expression of the empirical coefficients of hold-up (ϑ, η) and pressure drop (φ, ψ_1 or ξ, ζ). However, we have concluded that generally valid and sufficiently accurate relations for individual coefficients for packings of various diameters, shapes and for different flow rates and physical properties of phases cannot be expected. Accordingly, all these coefficients were eliminated from Eqs (*6*) and (*8*) and replaced by quantities that are more relevant to the process on the packing and can be therefore easily determined experimentally. For liquid hold-up and gas pressure drop in the range $G_{gk} \leqq G_g \leqq G_{gz}$ we have following relations

$$\left(\frac{G_g}{G_{gz}}\right)^2 \frac{\varrho_{gz}}{\varrho_g} = \frac{z^3 - z_e^3}{z_z^3 - z_e^3} \left(\frac{(e - z)\, z_z}{(e - z_z)\, z}\right)^3 , \tag{10}$$

$$\frac{\Delta P_g}{\Delta P_{gz}} = \frac{z^3 - z_e^3}{z_z^3 - z_e^3} \frac{z_z^3}{z^3} . \tag{11}$$

In the range $0 \leqq G_g \leqq G_{gk}$ then

$$\left(\frac{G_g}{G_{gk}}\right)^2 \frac{\varrho_{gk}}{\varrho_g} = \frac{z^3 - z_0^3}{z_k^3 - z_0^3} \left(\frac{(e - z)\, z_k}{(e - z_k)\, z}\right)^3 , \tag{12}$$

$$\frac{\Delta P_g}{\Delta P_{gk}} = \frac{z^3 - z_0^3}{z_k^3 - z_0^3} \frac{z_k^3}{z^3} . \tag{13}$$

For hold-up we have derived[8]

$$z_z/e = (z_e/e)^{3/4} . \tag{14}$$

For the extrapolated hold-up, z_e, and the hold-up in the loading point, z_k, we have found empirically on our packings[8]

$$(z_e/e) = 1{\cdot}044(z_0/e) - 0{\cdot}009, \quad z_k = 1{\cdot}041 z_0 . \tag{15), (16}$$

Equations (*1*)—(*16*) summarize all relations necessary in the following text. They also reflect the development of the problem as has been presented in preceding papers[1-8]. Although the correlations of the quantities z_0, G_{gz} and ΔP_{gz} for our packings have been made available, they are not shown here in order to underline the fact that Eqs (*9*)—(*14*) possess a more general character and form basic relations requiring additional information associated often with hard-to-define properties of liquid and packing (quality of the surface, forces acting between the packing and fluids *etc.*). The way in which the quantities z_0, G_{gz}, ΔP_{gz} were defined is not essential and may change from case to case. These quantities as well as the empirical relations (*15*) and (*16*) will certainly be subject to further development.

BUBBLE FLOW COLUMNS

As has been mentioned in the introduction this paper is an attempt to find relations between hydrodynamic characteristics of trickle and bubble flow columns which should lead to their unified description. This effort was motivated by the solution of an algebraic equation of the sixth order for the relative hold-up, z/e, Eq (*17*), which was given rise to by substituting numerical values for the coefficients ϑ and η and the mass velocities of phases, G_g and G_l, in Eq. (*8*)

$$\left(\frac{z}{e}\right)^6 - 3\left(\frac{z}{e}\right)^5 + 3\left(\frac{z}{e}\right)^4 - \left(1 + \frac{\vartheta G_l^2}{2g\varrho_l^2 d_e e^3} - \frac{\eta G_g^2}{2g\varrho_l\varrho_g d_e e^3}\right)\left(\frac{z}{e}\right)^3 + 3\frac{\vartheta G_l^2}{2g\varrho_l^2 d_e e^3}\left(\frac{z}{e}\right)^2 - 3\frac{\vartheta G_l^2}{2g\varrho_l^2 d_e e^3}\left(\frac{z}{e}\right) + \frac{\vartheta G_l^2}{2g\varrho_l^2 d_e e^3} = 0\,, \qquad (17)$$

or, in an abbreviated form and with the aid of Eq. (*14*) and (*9*) and the relative hold-up $\beta = z/e$

$$\beta^6 - 3\beta^5 + 3\beta^4 - \left[1 + \beta_z^4 - (1 - \beta_z)^4 (G_g/G_{gz})^2\right]\beta^3 + 3\beta_z^4\beta^2 - 3\beta_z^4\beta + \beta_z^4 = 0\,. \qquad (17a)$$

Six roots were obtained of which only two were usually real, the rest being conjugated. The real roots are shown in Fig. 1* for several liquid velocities. As it is apparent the dependence of liquid hold-up on gas velocity has two branches originating in the point β_z, G_{gz}. The lower branch represents the hold-up in a trickle bed as a function of velocity of counter-current gas, *i. e.* the case for which Eq. (*8*) was derived. The upper branch was speculatively interpreted as a dependence of the hold-up in a bubble flow column on the velocity of gas; gas being the discontinuous phase. If it is the case, then Eqs (*6*)–(*8*) would have to hold for the bubble flow regime with the same values of the empirical coefficients as those for the trickle bed. The constancy of the coefficients ξ, ζ, ψ_I and φ, however, is very unlikely. It may be expected, for instance, that the coefficient φ in a bubble flow bed will reach unity. Pertaining data for verification of our assumption were found in paper of Musil, Prost and LeGoff[9] and that of Bljachman and Jakubson[10] in graphical form.

Fig. 2 shows the experimental hold-up for water in a buble flow bed of Raschig rings 10·3 mm diameter as function of velocity of air taken over from Fig. 1 ref.[9]. Fig. 3 plots then the dimensionless gas pressure drop versus gas mass velocity as a log–log plot. A gradual increase of the exponent over the gas velocity is typical for trickle beds and it is often used to define some characteristic points: the loading

* Since only the real roots were needed, we found them easily from Eq. (*10*) by substituting various z for selected $z_e(z)$ and G_{gz}.

point and the upper and lower flooding points. The lower flooding point is shown in Fig. 3 by large circles, the upper one by dash-and-dot line. The hold-up and pressure drop curves in Figs 2 and 3 are continuous in the whole range of gas velocities pertaining to trickle and bubble flow beds. It is stressed, however, that the data for trickle and bubble flow beds were obtained independently and the curves shown in Figs 2 and 3 are combinations of corresponding branches for trickle and bubble flow beds. Clearly, it is not possible to proceed along the hold-up line for a trickle bed up to flooding, pass into the bubble flow regime by decreasing the flow rate of gas and reach ultimately the relative hold-up $\beta = 1$ at zero velocity of gas.

Figs 4–6 show the liquid hold-up and gas pressure drop from Figs 2 and 3 in terms of variables of Eqs (6)–(8) used earlier for processing the trickle bed data. In order that we may judge visually from Figs 2–6 the region in which the empirical coefficients (in Eq. (6) φ and ψ_1; in Eq. (7) ξ and ζ; in Eq. (8) ϑ and η) retain a constant value independent of gas velocity, the characteristic points are shown graphically.

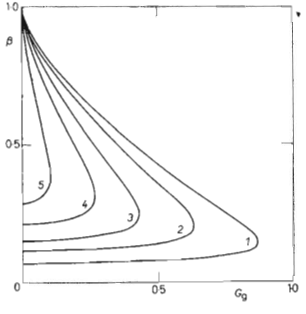

FIG. 1

Dependence of the Relative Hold-up on Gas Mass Velocity

The gas velocities of the flooding point and the coefficients ϑ and η are given in Table I. *1* $G_l = 1{\cdot}1\ \mathrm{kg\,m^{-2}\,s^{-1}}$, *2* 3·5, *3* 6·5, *4* 11·1, *5* 17·5.

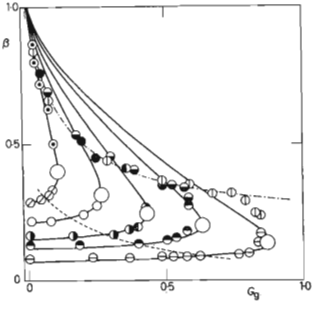

FIG. 2

Dependence of the Relative Hold-up under Trickle and Bubble Flow on Gas Mass Velocity

G_l (kg m^{-2} s^{-1})	1·1	3·5	6·5	11·1	17·5
trickle flow	⊖	◓	◑	○	⊘
bubble flow	⊕	◒	◐	●	⊙

Experimental data were taken from Musil, Prost, Le Goff[9] — Fig. 1. Full lines were computed from Eq. (10) by substituting z_e and G_{gz} from Table I. Broken line indicates the loading, large circles the lower flooding and dash-and-dot line the upper flooding points.

The values of loading point, computed from Eqs (*6*), (*10*) and (*16*), are indicated by broken line, the values of the lower flooding point, computed from Eqs (*6*), (*9*) and (*14*), by large circles, and the values of the upper flooding point (or a transition to the bubble flow regime), computed by setting $G_g = G_{gz}$ in a semiempirical equation (*18*) proposed by authors[9], are indicated by dash-and-dot line.

$$\beta = 1 - \frac{G_g/\varrho_g}{1{\cdot}23(G_g/\varrho_g - G_l/\varrho_l) + 0{\cdot}22e}. \qquad (18)$$

A very good linearity of the relations between the loading and lower flooding points $G_{gk} \leqq G_g \leqq G_{gz}$ under trickle flow is apparent from Figs 4–6. Corresponding empirical coefficients for individual liquid flow rates were evaluated graphically and may be found in Table I. A relatively satisfactory behaviour even below the loading point $0 \leqq G_g \leqq G_{gk}$ is evidenced by a good agreement of the experimental and calculated values of hold-up (see the full lines in Fig. 2 representing the computed hold-up *versus* gas mass velocity curve obtained by extrapolating the data from the region $G_{gk} \leqq G_g \leqq G_{gz}$). On transition to a bubble flow bed (upper flooding

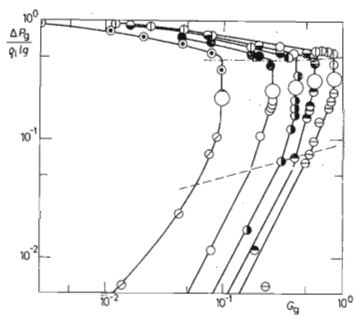

FIG. 3

Dependence of the Dimensionless Pressure Drop on Gas Mass Velocity in a log-log Plot

G_l (kg m^{-2} s^{-1})	1·1	3·5	6·5	11·1	17·5
trickle flow	⊖	◓	◑	●	⊘
bubble flow	ⓘ	◒	◐	○	⊙

Broken line indicates loading, large circles lower flooding and dash-and-dot line upper flooding points.

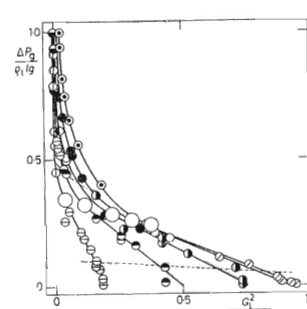

FIG. 4

Dependence of the Dimensionless Pressure Drop on $G_l^2/2g\varrho_l^2 d_e z^3$

G_l (kg m^{-2} s^{-1})	1·1	3·5	6·5	11·1	17·5
trickle flow	⊖	◓	◑	○	⊘
bubble flow	ⓘ	◒	◐	●	⊙

Broken line indicates loading, large circles lower flooding and dash-and-dot line upper points.

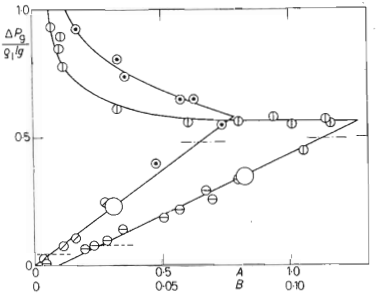

FIG. 5

Dependence of the Dimensionless Pressure Drop on $G_l^2/2g\varrho_g\varrho_l d_e(e-z)^3$

G_l (kg m^{-2} s^{-1})	1·1	17·5
abscissa	A	B
trickle flow	⊖	⊘
bubble flow	⊙	⊙

Broken line indicates loading, large circles lower flooding and dash-and-dot line upper flooding points.

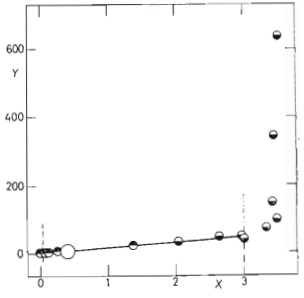

FIG. 6

Dependence of Liquid Hold-up on Gas Mass Velocity in Variables of Eq. (*8*) $Y = 2g\varrho_l^2 d_e z^3/G_l^2$, $X = (G_g/G_l)^2(\varrho_l/\varrho_g)\cdot(z/e-z)^3$, $G_l = 3{\cdot}5$ kg m^{-2} s^{-1}, ◓ trickle flow, ◒ bubble flow bed. Broken line indicates loading, large circles lower flooding and dash-and-dot line upper flooding points.

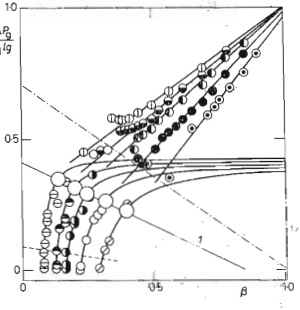

FIG. 7

Dependence of the Dimensionless Pressure Drop on the Relative Hold-up of Liquid

G_l (kg m^{-2} s^{-1})	1·1	3·5	6·5	11·1	17·5
trickle flow	⊖	◓	◑	○	⊘
bubble flow	⊙	◒	◐	●	⊙

Full lines were computed from Eqs (*6*) and (*19*) with the aid of the coefficients from Table I. Broken line indicates loading, large circles lower flooding and dash-and-dot line upper flooding points. Line *1* extrapolates the dependence of the lower flooding point, to zero hold-up and pressure drop.

TABLE I

Experimental and Computed Values of Some Characteristics of a Two-phase Flow of Liquid and Gas in Trickle and Bubble Flow Beds of Raschig Rings 10 mm Diameter — Data of Musil, Prost, Le Goff[9]

Two-phase flow characteristic	Liquid mass velocity G_l (kg m^{-2} s^{-1})				
	1·1	3·5	6·5	11·1	17·5
Trickle flow bed					
$\vartheta = 2g\varrho_l^2 d_e e^3 \beta_e^3 / G_l^2$	3·9	1·8	1·125	1·08	1·06
η	11·3	15·8	26·75	47·0	195·0
β_e	0·07108	0·1187	0·1535	0·2161	0·2912
β_z	0·1377	0·2022	0·2452	0·3169	0·3964
G_{gz} measured	0·853	0·591	0·429	0·260	0·097
G_{gz} computed from Eq. (*9*)	0·867	0·629	0·432	0·266	0·103
φ Eq. (*6*) — from Fig. 4	0·42	0·41	0·4	0·39	0·38
ψ_l Eq. (*6*) — from Fig. 4	2·1	0·82	0·526	0·426	0·402
$(\Delta P_{gz}/\varrho_l lg)$ computed from Eq. (*6*)	0·346	0·318	0·285	0·265	0·230
$(\Delta P_{gk}/\varrho_l lg)$ computed from Eq. (*6*)	0·0822	0·0987	0·0569	0·0546	0·0435
G_{gk} computed from Eq. (*10*)	0·625	0·449	0·296	0·151	0·055
β_k	0·08302	0·1349	0·1702	0·2283	0·3030
ξ from Fig. 5	4·75	—	—	—	75
ζ from Fig. 5	— 400	—	—	—	0
φ computed from Eq. (*5*)	0·416	—	—	—	1·64
ψ_l computed[5] from Eq. (*6*)	0·384	—	—	—	0·407
Bubble flow bed					
Re_l	2·45	7·8	14·5	24·7	39·0
$\psi_{l(\beta=1)} = 22·6/Re_l + 1·11$	9·24	3·66	2·48	1·91	1·61
$(\Delta P_l/\varrho lg)$; $(\beta = 1)$ Eq. (*3*)	0·00085	0·00341	0·008	0·0179	0·0376
k_1 from Fig. 7	0·279	0·181	0·108	0·076	−0·322
k_2 from Fig. 7	0·720	0·806	0·884	1·058	1·284
β_z^* Eq. (*18*)	0·299	0·332	0·378	0·449	0·624
$(\Delta P/\varrho_l lg)_z^*$ from Fig. 7	0·495	0·458	0·442	0·399	0·479

point), the courses given by Eqs (*5*)–(*7*) begin to depart from those for a trickle bed and further on display a non-linear character. That proves that a bubble flow bed cannot be described by Eqs (*6*)–(*8*) with constant, gas-velocity-independent empirical coefficients as has been done in the case of trickle flow. Thus a relatively good prediction of the relation between liquid hold-up and gas mass velocity under the bubble flow regime, and at high liquid flow rates in particular, is rather surprising (Fig. 2). In contrast, for low liquid flow rates, the calculated relation of liquid

hold-up and the mass velocity of gas begins to deviate from experimental data already in the lower flooding point. As follows from Eqs (*9*) and (*14*) at constant velocity of gas, this suggests that between the lower and upper flooding points the value of η decreases at simultaneous increase of the coefficient ϑ (and hence also the extrapolated hold-up z_e).

The dependences plotted in Figs 4–6 were not linear in the bubble flow region. On the other hand, a plot of the dimensionless pressure drop on the relative hold-up shown in Fig. 7 may be regarded as linear in this very region.

$$\frac{\Delta P_g}{\varrho_l g} = k_1 + k_2 \beta \,. \qquad (19)$$

Clearly, for a trickle flow bed the relation of pressure drop in these variables is strongly non-linear since it is described by Eq. (*6*), which for high relative hold-ups β approaches asymptotically the value of the coefficient φ. Fig. 7 further illustrates the decrease of pressure drop of the lower flooding point with increasing flow rate of liquid known from the literature. To verify the limiting points of this dependence,

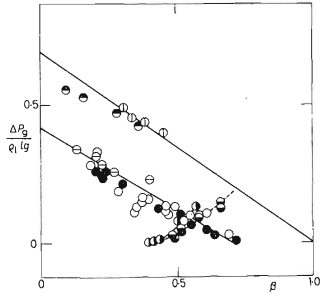

FIG. 8

Dependence of the Dimensionless Pressure Drop on the Relative Liquid Hold-up
Lower flooding point: 10 mm Raschig rings, ⊖ data of Musil[9], ○ this work; 10 mm glass spheres, ● this work. Upper flooding point: 10 mm Raschig rings, ⊙ data of Musil[9], ◓ Bljachman[10]. Dependence at $G_g = 0$. ◑ 10 mm Raschig rings, this work, ◒ 10 mm glass spheres, this work.

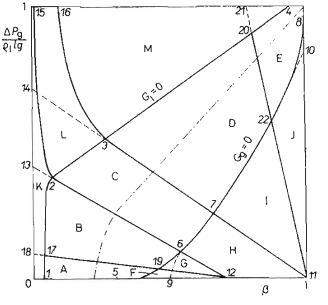

FIG. 9

Diagram of Regimes of a Two-Phase Flow in a Bed of 10 mm Raschig Rings

the measurement of pressure drop of the lower flooding point in a column 109·8 mm diameter packed with 10 mm Raschig rings and 10 mm glass spheres was carried out. The results are shown in Fig. 8 together with the data of Bljachman and Jakubson[10] obtained with 10 mm Raschig rings. From this figure it is apparent that starting from a certain flow rate of liquid the gas is being entrained by liquid. By blocking the escape route of gas below the supporting grid, the entrained gas has to travel back up through the packing giving rise to a pressure drop in the system with no gas supplied by the fan ($G_g = 0$). The intersect of the curve for the lower flooding point and that for zero velocity of gas ($G_g = 0$) in Fig. 8 designates the point of flooding (*i.e.* a point where a thin layer of liquid appears above the packing) at zero velocity of gas. The end point of the curve of the lower flooding points at zero pressure drop

TABLE II

Characteristic Points of a Two-Phase Flow of Liquid and Gas in a Trickle and Bubble Flow Bed

Point	G_l	G_g	β	$\Delta P_g/\varrho_l l_g$
1 Static hold-up of liquid in a trickle flow bed	0	0	0·039	0
2 Flooding point of a trickle bed at zero velocity of liquid	0	2·24	0·075	0·38
3 Flooding point of a bubble flow bed at zero velocity of liquid	0		0·27	0·52
4 Static hold-up of liquid in a bubble flow bed	0	0	0·95	1
5 Onset of entrainment of liquid by gas in a trickle flow bed	~17	≦0	~0·3	0
6 Flooding point in a trickle flow bed at zero velocity of gas	~38	0	0·535	0·10
7 Flooding point in a bubble flow bed at zero velocity of gas	~38	0	0·67	0·23
8 Onset of entrainment of gas by liquid in a bubble flow bed	~17	≦0	1	0·962
9 Liquid hold-up in trickle flow bed with removal of entrained gas at zero gas velocity and such velocity of liquid which causes flooding unless the gas is removed	38	<0	~0·5	0
10 Pressure drop computed from the resistance to a single-phase flow of liquid at a rate which causes flooding of a bubble flow bed at zero velocity of gas	38	≦0	1	0·85
11 Single-phase "critical" velocity at which the pressure drop equals the driving force	104	0	1	0
12 Lower flooding point of a trickle bed at zero gas pressure drop	70	<0	0·7	0

$\Delta P_{gz}/\varrho_l lg = 0$ may be interpreted as giving mass velocity of liquid at which the resistance due to friction between the liquid on one hand and the gas and the surface of the packing on the other hand equals the driving force. The other end point, $(\Delta P_{gz}/\varrho_l lg)_{\beta=0} = 0{\cdot}41$, may be regarded as a pressure drop of the lower flooding point extrapolated to zero hold-up of liquid. A similar curve, obtained with the aid of Eq. (*18*), is drawn for the bubble flow regime and determines completion of the transition to a bubble flow bed.

From the already discussed curves in Figs 2–8 it follows that the bubble flow regime cannot be described by mere interpolation of the relationships for trickle flow with constant values of empirical coefficients. Liquid hold-up and gas pressure drop are not linear in terms of variables of Eqs (*6*)–(*8*). However, from the conti-

TABLE I
(*Continued*)

Point	G	G		P
13 Pressure drop of the flooding point in a trickle bed extrapolated to zero hold-up	0	2·32	0	0·41 Fig. 6
14 Pressure drop of the flooding point in a bubble flow bed extrapolated to zero hold-up	0	3·05	0	0·7
15 Hold-up of a wet layer at unit dimensionless pressure drop	0	—	choice 0·01	1
16 Hold-up of a bubble flow bed at unit dimensionless pressure drop	0	—	choice 0·1	1
17 Pressure drop of the loading point in a trickle bed at zero velocity of liquid	0	1·055	0·0406	0·086
18 Pressure drop of the loading point in a trickle bed extrapolated to zero hold-up	0	1·062	0	0·092
19 Loading point of a trickle bed at zero velocity of gas	29	0	0·465 Fig. 9	0·032
20 Point of transition of a bubble flow bed from the regime of flow of individual free bubbles to the flow of bubble clusters at zero velocity of liquid	0	0·022	0·81	0·9
21 Point of transition of a bubble flow bed from the regime of flow of individual free bubbles to the flow of bubble clusters extrapolated to unit pressure drop	0	—	0·74 Fig. 9	1
22 Point of transition of a bubble flow bed from the regime of flow of individual free bubbles to the flow of bubble clusters at $G_g = 0$	—	0	0·875	0·57

nuity of the curves in the transition region follows the continuity of the descriptions of trickle and bubble flow beds. In case of pressure drop it is the transition from Eq. (*6*) to a form given in Eq. (*19*). Such description will be attempted in the following. First, however, we shall generalize the situation depicted in Figs 7 and 8 and construct a diagram of regimes of a two-phase flow of liquid and gas in a bed of packing.

The Diagram of Regimes of a Two-Phase Flow of Liquid and Gas in a Bed of Packing

Fig. 9 is a diagram of regimes indicating individual regimes and characteristic points of a two-phase flow of liquid and gas in a trickle and bubble flow bed. The ranges of gas pressure drop and liquid hold-up are respectively $0 \leqq \Delta P/\varrho_l lg \leqq 1$ and $0 \leqq \beta \leqq 1$. The diagram of regimes was drawn for a packing of Raschig rings 10 mm diameter using data of authors[9,10] and our own measurements. It is assumed that the packing is fixed on top by a grid to prevent its motion and that the resistance of the supporting grid to the flow of gas and liquid is negligible. The distribution of liquid and gas is assumed uniform both in space and time. The data on gas pressure drop and liquid hold-up from outside the operating region of counter-current trickle and bubble flow beds are lacking and the existence of individual regimes is only a speculation based on observation and physical reasoning. Accordingly, the existence of certain regimes as well as the position of some characteristic points or lines may be corrected by future experiments.

The lines $\beta = 0$ and $\beta = 1$ in Fig. 9 represent respectively the dimensionless pressure drop of a single-phase flow of gas $\Delta P_g/\varrho_l lg = \Delta P/\varrho_l lg$ and liquid $\Delta P_l/\varrho_l lg = 1 - \Delta P/\varrho_l lg$. The abscissa gives the hold-up for various flow rates of liquid. The lower left hand corner of Fig. 9 comprises a region where the discontinuous phase is liquid; in the upper right hand corner the continuous phase is liquid. Point *1* in Fig. 9 marks the static hold-up of a trickle bed at zero flow rate of liquid. Its value may be calculated from a number of correlations or determined experimentally. Point *2* represents the flooding point of the bed at zero flow rate of liquid. This point can be approached experimentally by increasing the velocity of gas and simultaneous decreasing the flow rate of liquid. Point *3* indicates the upper flooding point or the terminal point of a transition to a bubble flow bed. The abscissa of the point *4* ($\Delta P/\varrho_l lg = 1$) may be generally smaller than unity providing that after closing the supply of gas into the bubble flow bed its static gas hold-up remains in the bed. Point *4* is thus an analogue of the static hold-up of liquid in a trickle flow bed (Point *1*). By increasing the flow-rate of liquid in a trickle bed the hold-up increases and we move along the axis of the dimensionless hold-up β at $\Delta P_g/\varrho_l lg = 0$. Having reached a certain flow rate of liquid a marked entrainment of gas by liquid occurs ($G_g < 0$) — point *5*. If the entrained gas is not allowed to escape through the supporting grid ($G_g = 0$), it returns upwards causing a certain pressure drop arcross the bed to appear. By further increase of the liquid flow rate the pressure drop increases reaching at $G_{gz} = 0$ the first flooding point in point *6* where a thin layer of liquid forms on top of the packing. Point *7* is again a terminal point in transition to a bubble flow bed. Following the zero gas velocity line ($G_g = 0$) at simultaneous decrease of liquid flow rate we reach point *8* at $\beta = 1$. This point determines that single-phase liquid flow rate at which each bubble of gas introduced into the stream is pulled down below the supporting grid. The ordinate of this point then depends on the size of these bubbles. Point *9* marks the liquid hold-up at zero pressure drop in case when the entrained gas is being removed ($G_g < 0$). The liquid flow rate of this point would cause flood in ginpoint *6* if the entrained gas was forced to remain in the bed. Point *10* is determined by pressure drop of a single-phase flow of liquid at rates corresponding to points *6*, *7* and *9*. With the rate of liquid under single-phase

flow further increasing we approach point *11* until reaching the state when the pressure drop of liquid at $\beta = 1$ equals the driving force. This critical flow rate may be calculated from an equation for the resistance under single-phase flow through the bed of packing, *e.g.* the Ergun equation[11]. On proceeding now from point *6* along the line of the lower flooding point and increasing the liquid flow rate we have to withdraw an increasing amount of entrained gas from below the supporting grid. The pressure drop necessary to reach the lower flooding point is thus decreased until in point *12* it reaches zero. The line of the lower flooding point would terminate in point *11* ($\beta = 1$, $\Delta P_g/\varrho_l lg = 0$) for a packing of such geometric shape which would not permit the bubbles of entrained gas to stay within the pockets of packing by the action of capillary forces. For a packing of Raschig rings 10 mm diameter we have observed that a part of the gas does remain trapped within the rings having their axis close to a horizontal level. A relatively large number of bubbles were retained in the packing even with the height of liquid reaching 10 cm above the top. The bubbles will leave their traps only after the pressure fluctuations of liquid have exceeded the value of interfacial tension. It is apparent that of prime importance are the size, the shape and orientation of a piece of packing, the surface tension and the contact angle. In case of the upper flooding point line the location of the terminal point on the beta axis at $\Delta P_g/\varrho_l lg = 0$ is determined by the history of the packing. Let us suppose that we start from a single-phase flow of liquid at $\beta = 1$ from point *11* and introduce bubbles of gas into the bed. The bubbles will be pulled below the supporting grid and it is very unlikely that any of them would penetrate into the voids displacing the liquid and remaining there. On the other hand, when starting with a bubble flow bed at low holds-ups of liquid and increasing the flow rate of liquid the same situation as that described in connection with the lower flooding point will occur and the terminal point will appear somewhere between points *12* and *11*. For this uncertainty we shall regard point *11* as the terminal point of the upper flooding point line. From Figs 7 and 8 it is seen that in region $G_1 \geqq 0$ the upper and lower flooding point lines, delimiting the transition to a bubble flow bed, may be approximated by straight lines. Extrapolating these straight lines to zero hold-up, $\beta = 0$, points *13* and *14* are obtained. The pressure drop of a dry packing in point *13* may be calculated from the gas mass velocity of the lower flooding point extrapolated from point 2 G_{gz} ($G_1 = 0$) to zero liquid hold-up G_{gz} ($\beta = 0$). The extrapolated pressure drop in point *14* (read off from Fig. 7) for a bed of Raschig rings is given in Table II. The extension of the lines for the upper and lower flooding points at $G_1 \leqq 0$ leads to points *15* and *16* giving rise to the regime of gas flow through a wet layer of packing — K ($G_1 = 0$), the transport of entrained liquid by gas — L ($G_1 < 0$), non-stationary bubble flow regime at $G_1 = 0$, or the transport of liquid by bubbling gas M — ($G_1 < 0$).

There are two principal definitions of the loading point existing in the literature[12]. The first definition utilizes a log-log plot of the pressure drop versus gas mass velocity. The pressure drop of the loading point in these plots increases with increasing flow rate of liquid, while the pressure drop of the flooding point decreases. From this it follows that the flooding and the loading points should coincide at a certain gas mass velocity $G_g > 0$. The other definition of the loading point is based on the dependence of hold-up on gas velocity. A defined increment of hold-up in comparison with the hold-up at zero pressure drop across the layer is taken for definition of the loading point (an increased interaction between the gas and liquid). The pressure drop of the loading points decreases with the velocity and it may be easily defined even for negative gas velocities in region F. Here it is assumed that the loading point at zero pressure drop is reached in point *12*. Provided that the relation is linear the points *17* and *18* represent the pressure drops of the loading points extrapolated to zero flow rate of liquid and zero hold-up. Point *19* is then the loading point at zero gas velocity $G_{gk} = 0$. Similarly as for trickle beds, where the loading point marks the change of regime, an analogous transition of regimes may be expected in case of the bubble flow bed. The authors[10] observed a transition from the regime of flow of individual

free bubbles to a pulsation regime characterized by clusters of bubbles (larger bubbles) rising at a velocity greater that that of free motion of bubbles. The hold-up of the transition between these two types of bubble flows, point *20*, was estimated from data[10]. Point *21* is an extrapolation of this point to unit dimensionless pressure drop; point *22* is its intersect with the $G_g = 0$ line.

The above mentioned characteristic points are defined by the regimes of a two-phase flow of liquid and gas in trickle and bubble flow beds:

A (*1,5,19,17,1*) Trickle flow bed with counter-current flow of gas below the loading point.

B (*17,19,6,2,17*) Trickle flow bed with counter-current flow of gas between the loading and flooding points.

C (*2,6,7,3,2*) Transition regime between a trickle and a bubble flow bed.

The transition region is delimited by the lower and upper flooding points. These points differ primarily in their pressure drop and hold-up and their gas velocity is constant or changes only very little. Our experimental runs ended usually in the lower flooding point by formation of a thin layer of foam or liquid on top of the packing. By increasing the flow rate of liquid the layer grows. If, however, the flooding is initiated in the vicinity of the supporting grid, the upper flooding point is reached. The onset of flooding near the grid is probably caused by diminished free cross-section available to the flow of gas due to the presence of the grid, by lower local porosity or by imperfect conditions for draining. We have observed that high flow rates of liquid tend to reach the upper flooding point. In contrast, for lowest liquid flow rates and packings of large size or high porosity difficulties with entrainment occur already below the lower flooding point.

D (*3,7,20,22,3*) Bubble flow bed with counter-current flow of gas in the form of clusters of bubbles.

E (*20,22,8,4,20*) Bubble flow bed with counter-current flow of gas in the form of individual free bubbles.

F (*5,9,12,19,5*) Trickle flow bed with co-current flow of entrained gas below the loading point.

G (*19,12,6,19*) Trickle flow bed with co-current flow of entrained gas between the loading and flooding points.

Eqs (*10*) and (*12*) do not hold in regions F and G with the original meaning of gas mass velocity, G_g, defined as the amount supplied by the fan. It should be realized that the amount transported by liquid from top of the packing below the grid suffices to flood the packing.

H (*6,12,11,7,6*) Transition region.

I (*7,11,22,7*) Bubble flow with co-current flow of gas in the form of clusters of bubbles.

The bubbles introduced into the layer are transported below the supporting grid. If they are not allowed to escape with the liquid, or if the gas is supplied below the grid by a distributor, the gas will accumulate and having reached a sufficient volume a bubble (slug) will pass through the packing giving rise to a strongly non-stationary regime.

J (*11,10,8,22,11*) Bubble flow bed with co-current flow of entrained gas in the form of individual free bubbles. A non-stationary regime occurs if the gas is supplied below the grid or the entrained bubbles are not being withdrawn.

K (*1,17,2,15,14,13,18,1*) Wet packing and counter-current flow of gas at zero flow rate of liquid.

L (*2,3,16,15,2*) Liquid transported by gas as carry-over.

M (*3,20,4,21,16,3*) Transport of liquid upwards ($G_l < 0$) by bubbling gas, or non-stationary bubble flow bed at $G_l = 0$.

The diagram of regimes, aside from its particular validity for a packing of porcelain Raschig rings 10 mm diameter, pertains also generally to a two-phase flow through a bed of packing. Its general character rests in defining individual regimes and characteristic points. The dash-and-dot line in the diagram gives the dependence of pressure drop on liquid hold-up at $G_l = 11{\cdot}1$ kg . m^{-2} s^{-1} taken from Fig. 7.

Theoretical Analysis of a Two-Phase Flow in Trickle and Bubble Flow Beds

Two qualitatively different regimes – the trickle and the bubble flow – were depicted jointly in the diagram of regimes in Fig. 9 with the dimensionless pressure drop and the relative hold-up as variables. The experimental courses of pressure drop, described by different relations (Eq. (*6*) and (*19*)), transform in region C continuously from one regime into the other. We shall therefore attempt a unified theoretical analysis of a two-phase flow of liquid and gas in trickle and bubble flow beds. As before, the analysis starts from basic macro-balances of momentum and vertical components of forces acting on the liquid stream. In the derivation we shall retain all assumptions listed in the original paper[1] on trickle flow bed. Unlike Musil and coworkers[9] we shall admit direct contact of gas bubbles with the surface of packing. This assumption is regarded necessary not only for description of the static hold-up of gas trapped in the packing at zero flow rates of both phases, but, above all, for the two-phase flow through the packing. At the same time we believe that the volume forces of liquid transmitted onto the packing either directly as a consequence of the geometry of the packing or through the surface forces, cannot be expressed solely in terms of the static hold-up of gas or liquid. At the two-phase flow these forces are apparently greater and for a given flow rate of liquid change with the velocity of gas.

A principal difference between trickle and bubble flow beds rests in the fact that in trickle beds the discontinuous phase is liquid, while in bubble flow beds it is the gas. The balance of the vertical components of forces acting on the liquid and gas in a trickle bed $(i = 1, j = 0)$ and a bubble flow bed $(i = 0, j = 1)$ then contains only the terms the presence of which depends on whether the liquid phase is continuous $(i = 0)$, or discontinuous $(i = 1)$. The balance in joint notation takes then the following form

for liquid:

$$Ae\beta\,\Delta P = e\beta\varrho_l g Al - \tau_{ls} a_{ls} Al - \tau_{lg} a_{lg} Al - iF_l\,, \qquad (20)$$

for gas:

$$Ae(1-\beta)\,\Delta P = e(1-\beta)\,\varrho_g g Al + \tau_{lg} a_{lg} Al + \tau_{gs} a_{gs} Al + jF_g\,, \qquad (21)$$

where the intensive quantities are averaged in time and over the volume of the layer $A.\,l.$ τ_{ls} is the vertical component of friction between the liquid stream and the surface of packing and τ_{lg} is the vertical component of friction between the gas and the liquid stream. τ_{gs} is the vertical component of friction in the gas stream brought about

by changes of direction, contraction and expansion as well as by friction in contact with dry surface of packing, which cannot be expressed as friction between the gas and liquid streams (τ_{lg}) .a_{ls}, a_{lg}, a_{gs} are corresponding specific surfaces related to a unit volume of the bed. F_l and F_g denote the volume forces of liquid and gas supported by the packing owing to the peculiarities of its shape and orientation in the bed and as a consequence of the surface tension forces. By adding Eqs (*20*) and (*21*) we obtain after some arrangement

$$\frac{\Delta P}{\varrho_l l g} = \beta + (1 - \beta)\frac{\varrho_g}{\varrho_l} - \frac{\tau_{ls} a_{ls}}{e\varrho_l g} + \frac{\tau_{gs} a_{gs}}{e\varrho_l g} - \frac{iF_l}{e\varrho_l g A l} + \frac{jF_g}{e\varrho_l g A l} . \qquad (22)$$

On the left hand side of Eq. (*22*) there is the experimentally found pressure drop and the experimental hold-up on the right hand side. The friction stresses τ_{ls} and τ_{gs} and the corresponding specific surfaces have to be calculated or estimated also as a fraction of the volume forces of liquid, F_l, or gas, F_g, transmitted onto the packing. These are expressed by means of the coefficients φ' and φ^* as follows

$$\frac{F_l}{e\varrho_l g A l} = (1 - \varphi')\beta ; \quad \varphi' \geqq 0 \quad \text{for} \quad G_l \geqq 0 , \qquad (23)$$

$$\frac{F_g}{e\varrho_l g A l} = (\varphi^* - 1)\beta ; \quad \varphi^* \geqq 1/\beta_{G_g = G = 0} \quad \text{for} \quad G_l \geqq 0 . \qquad (24)$$

As it is apparent from Eq. (*22*), liquid hold-up at constant pressure drop will be the lower the higher the value of the term containing τ_{gs}. The vertical component of friction due to the changes of direction, contraction and expansion and perhaps due to friction with the dry surface of the packing does not increase the hold-up. However, τ_{gs} takes different values not only in trickle and bubble flow beds but it varies also with the flow rate of liquid. In order that we may assess the effect of the relative magnitude of the terms containing τ_{gs} and τ_{gl} on the relation of pressure drop and hold-up, we shall define the friction between the liquid and the gas stream by means of a fraction x and the following equation

$$\frac{\tau_{gl} a_g}{e\varrho_l g} = x\left[(1 - \beta)\left(\frac{\Delta P}{\varrho_l l g} - \frac{\varrho_g}{\varrho_l}\right) - j(\varphi^* - 1)\beta\right]; \quad 0 \leqq x \leqq 1 . \qquad (25)$$

For the term expressing the losses due to changes of direction, contraction and expansion, we obtain with the aid of Eq. (*21*) the following relation

$$\frac{\tau_{gs} a_{gs}}{e\varrho_l g} = (1 - x)\left[(1 - \beta)\left(\frac{\Delta P}{\varrho_l l g} - \frac{\varrho_g}{\varrho_l}\right) - j(\varphi^* - 1)\beta\right]; \quad 0 \leqq x \leqq 1 . \qquad (26)$$

On substituting from Eqs (*23*), (*24*) and (*26*) into (*22*) we obtain finally

$$\frac{\Delta P}{\varrho_l l g} = \frac{\beta[1 + jx(\varphi^* - 1) - i(1 - \varphi')] + (1 - \beta)(\varrho_g/\varrho_l)}{\beta + x(1 - \beta)} - \frac{1}{\beta + x(1 - \beta)} \frac{\tau_{ls} a_{ls}}{e \varrho_l g} . \tag{27}$$

The derived general equation (*27*) for the description of the pressure drop in trickle and bubble flow beds contains parameters x, φ', φ^* and $\tau_{ls} a_{ls}$. The expected variations of the fraction x and the parameters φ' and φ^* accompanying the change of regime and liquid flow rate are the cause why the pressure drop in trickle and bubble flow beds cannot be described by a relation with constant coefficients. The given parameters cannot be evaluated from experimental data without additional assumptions. For instance, the requirement of dividing the pressure drop between the contribution of the gas–liquid friction (x) and that due to changes of direction, contraction and expansion is quite demanding. One has to realize that even the single-phase flow through the bed has not been quite satisfactorily described, and the less so the part of the resistance due to skin friction. Only recently the single-phase flow in model beds of identical spheres has been studied in more detail.

Some limiting solutions of Eq. (*27*) will be shown in the following. On neglecting the term $(1 - \beta)\,\varrho_g/\varrho_l$, Eq. (*27*) may be written for a trickle bed ($i = 1, j = 0$) as

$$\frac{\Delta P}{\varrho_l l g} = \frac{\beta\varphi'}{\beta + x(1 - \beta)} - \frac{1}{\beta + x(1 - \beta)} \frac{\tau_{ls} a_{ls}}{e \varrho_l g} \tag{28a}$$

and for a bubble flow bed ($i = 0, j = 1$) as

$$\frac{\Delta P}{\varrho_l l g} = \frac{\beta[x(\varphi^* - 1) + 1]}{\beta + x(1 - \beta)} - \frac{1}{\beta + x(1 - \beta)} \frac{\tau_{ls} a_{ls}}{e \varrho_l g} . \tag{28b}$$

The fraction x, denoting the gas-liquid friction, appears also in Eqs (*28a,b*). It can be shown that below the loading point and under low liquid flow rates no visible interaction between gas and the trickling liquid occurs. This follows both from weak correlation between liquid hold-up and gas velocity, and from a plot of the friction coefficient versus gas Reynolds number which has a similar course as that for the dry packing. As a first approximation we may therefore assume that the magnitude of the gas–liquid friction will correspond to the skin friction on the surface of the packing at single-phase flow. Wentz and Thodos[12] reported the friction losses in a bed of spheres equal 12%. For a packing of irregular shape, such as *e.g.* Raschig rings, this value will be apparently even lower. On setting $x = 0$ in Eq. (*28a*) we obtain

$$\frac{\Delta P}{\varrho_1 l g} = \varphi' - \frac{1}{\beta}\frac{\tau_{1s} a_{1s}}{e\varrho_1 g} . \tag{29}$$

Assuming that $a_{1s} = a$ and after substituting

$$\tau_{1s} = k\varrho_1 u_1^2/2 \tag{30}$$

we arrive at the relation

$$\frac{\Delta P}{\varrho_1 l g} = \varphi' - kG_1^2/2g\varrho_1^2 d_e e^3 \beta^3 , \tag{31}$$

which has the form of Eq. (6).

For a bubble flow bed at low velocities of gas and high liquid hold-ups – regime E – a principal part of the resistance to flow is offered by the gas–liquid friction.

Accordingly, setting $x = 1$ in Eq. (28b) we obtain

$$\frac{\Delta P}{\varrho_1 l g} = \varphi^* \beta - \frac{\tau_{1s} a_{1s}}{e\varrho_1 g} . \tag{32}$$

On comparing Eq. (32) with the empirical Eq. (19), evaluated on the basis of Fig. 7, we obtain an equation for the coefficient φ^* in the following form

$$\varphi^* = k_2 + \frac{k_1}{\beta} + \frac{1}{\beta}\frac{\tau_{1s} a_{1s}}{e\varrho_1 g} . \tag{33}$$

Unfortunately, Eq. (33) contains a term with the unknowns τ_{1s} and a_{1s}. To evaluate φ^* one would therefore have to know the dependence of $\tau_{1s} a_{1s}/e\varrho_1 g$ on the hold-up β, or to assume a_{1s} equal the total surface ($a_{1s} \equiv a$), and to evaluate the friction stress from data on single-phase flow of liquid. If, however, $k_1 = -\tau_{1s} a_{1s}/e\varrho_1 g$ the coefficient $\varphi^* \equiv k_2$ and it is therefore independent of gas velocity. This will be probably true even for some higher liquid flow rates as follows from values of the coefficients k_1 and k_2 in Table I.

From the presence of the coefficient φ^* in Eq. (32) (by definition $\varphi^* > 1$) it further follows that it is not necessary for the friction stress τ_{1s} to be negative as reported by authors[9] at lower flow rates of liquid. This physically very unlikely conclusion was apparently drawn from the assumption excluding the contact of gas bubbles with the surface of packing. In other words, the authors did not assume that the wall may counterbalance a part of the volume forces of gas either directly or through the action of surface forces between the phases.

From the derived general expression for description of trickle and bubble flow beds Eq. (27), and on the basis of the above mentioned assumptions regarding the

gas–liquid friction we have obtained Eqs (*31*) and (*32*). Furthermore, the conditions were shown under which these equations transform into simple limiting expressions (*6*) and (*19*), the validity of which has been empirically verified. In case of a trickle flow bed the various non-zero average values of the fraction under the regime below and above the loading point are apparently the cause of various empirical coefficients evaluated experimentally from Eqs (*6*) and (*8*) in regions $0 \leqq G_g \leqq G_{gk}$ and $G_{gk} \leqq G_g \leqq G_{gz}$.

LIST OF SYMBOLS

a	specific surface of packing (m^{-1})
A	cross-section of bed (m^2)
$d_e = 1/a$	characteristic diameter of packing (m)
e	porosity
F	volume force of liquid transmitted onto packing (N)
g	acceleration due to gravity (ms^{-2})
G	mass velocity of fluid ($kg\ m^{-2}\ s^{-1}$)
i, j	constants defined in text
k, k_1, k_2	empirical constants
l	height of bed (m)
ΔP	resistance of bed ($N\ m^{-2}$)
$\mathrm{Re} = Gd_e/\mu$	Reynolds number
x	fraction defined in Eq. (*25*)
z	liquid hold-up per unit volume
$\beta = z/e$	relative hold-up
φ	empirical coefficient defined in Eq. (*4*)
φ'	empirical coefficient determining the volume forces of liquid transmitted onto packing, defined in Eq. (*23*)
φ^*	empirical coefficient determining the volume forces of gas transmitted onto packing, defined in Eq. (*24*)
ϑ, η	coefficients in Eq. (*8*)
ψ	friction factor
ξ	empirical coefficient in Eq. (*7*)
ζ	empirical coefficient in Eq. (*7*) ($N\ m^{-3}$)
ϱ	density ($kg\ m^{-3}$)
μ	viscosity ($N\ s\ m^{-2}$)
σ	surface tension ($N\ m^{-1}$)
τ	friction stress ($N\ m^{-2}$)

Subscripts

b	transition point from flow of individual free bubbles to flow of clusters of bubbles
e	extrapolated value
k	loading
o	value at $\Delta P_g = 0$
s	packing
st	static
z	flooding

REFERENCES

1. Kolář V., Brož Z.: This Journal *30*, 2527 (1965).
2. Brož Z., Kolář V.: This Journal *33*, 349 (1968).
3. Brož Z., Kolář V.: This Journal *33*, 2722 (1968).
4. Kolář V., Tichý J.: This Journal *33*, 2728 (1968).
5. Kolář V., Brož Z.: This Journal *33*, 3870 (1968).
6. Kolář V., Brož Z., Tichý J.: This Journal *35*, 3344 (1970).
7. Kolář V., Brož Z.: This Journal, in press.
8. Brož Z., Kolář V.: This Journal, in press.
9. Musil L., Prost C., Le Goff P.: Chim. Ind. *100*, 674 (1968).
10. Bljachman L. I., Jakubson A. M.: *Processy Chimičeskoj Technologii* (*Gidrodinamika, Teplo- i Masoperedača*). Sbornik Statej Akad. Nauk SSSR, p. 67. Moscow 1965.
11. Ergun S., Orning A. A.: Ind. Eng. Chem. *41*, 1179 (1949).
12. Buchanan I. A.: Ind. Eng. Chem. Fund. *6*, 401 (1967).
13. Wentz C. A., Thodos G.: A.I.C.H.E.J. *9*, 359 (1963).

Translated by V. Staněk.